Multi-objective Hierarchic Memetic Solver for Inverse Parametric Problems *

Ewa Gajda-Zagórska[1], Maciej Smołka[1], Robert Schaefer[1], David Pardo[2,3,4], and Julen Álvarez-Aramberri[2,3,5]

[1] Department of Computer Science, AGH University of Science and Technology, Kraków, Poland, {gajda,smolka,schaefer}@agh.edu.pl,
[2] Department of Applied Mathematics, Statistics, and O. R., University of the Basque Country (UPV/EHU), Leioa, Spain {dzubiaur,julen.alvarez.aramberri}@gmail.com
[3] Basque Center for Applied Mathematics (BCAM), Bilbao, Spain
[4] Ikerbasque (Basque Foundation for Sciences), Bilbao, Spain
[5] University of Pau (UPPA), France

Abstract
We propose a multi-objective approach for solving challenging inverse parametric problems. The objectives are misfits for several physical descriptions of a phenomenon under consideration, whereas their domain is a common set of admissible parameters. The resulting Pareto set, or parameters close to it, constitute various alternatives of minimizing individual misfits. A special type of selection applied to the memetic solution of the multi-objective problem narrows the set of alternatives to the ones that are sufficiently coherent. The proposed strategy is exemplified by solving a real-world engineering problem consisting of the magnetotelluric measurement inversion that leads to identification of oil deposits located about 3 km under the Earth's surface, where two misfit functions are related to distinct frequencies of the electric and magnetic waves.

Keywords: inverse problems, multi-objective optimization methods, memetic algorithms

1 Introduction

Parametric inverse problems (IPs) for partial differential equations (PDEs) play a crucial role in numerous tasks in science, technology and medicine. There exist a variety of applications of

*The work presented in this paper has been partially supported by Polish National Science Centre grants no. DEC-2012/07/B/ST6/01229, DEC-2012/05/N/ST6/03433, and DEC-2011/03/B/ST6/01393, D. Pardo and J. Álvarez-Aramberri were partially funded by the RISE Horizon 2020 European Project GEAGAM (644602), the Project of the Spanish Ministry of Economy and Competitiveness with reference MTM2013-40824-P, the BCAM Severo Ochoa accreditation of excellence SEV-2013-0323, the CYTED 2011 project 712RT0449, and the Basque Government through the BERC 2014-2017 program and the Consolidated Research Group Grant IT649-13 on "Mathematical Modeling, Simulation, and Industrial Applications (M2SI)".

IPs, including oil and gas exploration, structure health monitoring, and cancer tissue diagnosis (see *e.g.* [19]). Typically, parametric inverse problems are formulated as global optimization problems (GOPs), where the decision variables are induced by discrete representations of the unknown parameter functions. The misfit between measurement and simulated PDE solutions stands for the GOP's objective functional. Numerical IPs solvers encounter multiple challenges, generally caused by the ill-conditioning and non-uniqueness of the solution (multi-modality). Misfit regularization (see *e.g.* [8]) and the use of complex stochastic searches (see *e.g.* [12]) allow to overcome difficulties caused by mathematical model imperfections and numerical errors, but neither of these approaches can handle the lack of data or its inappropriate utilisation.

The following multi-objective approaches for solving IPs might be found in the literature:
A. *Multiple misfit functions obtained for multiple physics.* In particular, the authors of [3] apply the inverse quantitative structure-property relationship for designing new chemical compounds. Optimal design of a magnetic pole is considered in [5]. Here, different objective functions are associated with two independent methods of solving the considered forward problem.
B. *Multi-objective analysis used to improve the conditioning of the solving method.* A two-objective parameter identification using a genetic algorithm is reported in [15]. The second additional criterion was used to penalize populations with small diversity. Another approach, used, *e.g.*, in [6], was to combine two objective function formulations with an immunological algorithm. The two objective functions modelled fitnesses of individuals and T-cells, respectively.

The strategies presented in this paper fall into the first group (A). Let us assume that we can observe n physical processes $u^i(\omega) \in V^i$, $i = 1, \ldots, n$, which depend on the unknown parameter $\omega \in \mathcal{D}$, where V^i are proper Sobolev spaces. Let $A^i(u^i(\omega)) = 0$ be the relevant governing equations, where $A^i : V^i \longrightarrow (V^i)'$ is a family of differential operators from V^i to their conjugate. We assume to know d, the vector of state observations $d^i \in \mathcal{O}^i$ and introduce the vector of misfit functionals $f(d, u(\omega))$ with coordinates $\mathcal{O}^i \times \mathcal{D} \ni (d^i, u^i(\omega)) \to f^i(d^i, u^i(\omega)) \in \mathbb{R}_+$, associated with particular physics $i = 1, \ldots, n$.

The inverse problem formulated as the multi-objective problem consists of finding parameters ω such that they minimize all misfit functionals in the Pareto sense (see *e.g.* [14])

$$\min_{\omega \in \mathcal{D}} \{ f(d, u(\omega)) : \ A(u(\omega)) = 0 \}, \tag{1}$$

where $A(u(\omega)) = 0$ is the system of equations $A^i(u^i(\omega)) = 0$, $i = 1, \ldots, n$.

In this work, we analyze, whether such multi-objective approach, introduced in [11] allows to develop algorithms with two important features. First, increased robustness, which in particular leads to improved guarantee of finding a solution. Second, reduced computational cost, which results from improved conditioning. The presented approach utilizing two (or more) physical models aims at reducing the number of unwanted solutions by comparing the objectives results and preferring similar solutions.

In this paper, we apply the complex, multi-deme Hierarchic Memetic Strategy (HMS) [17] especially designed to solve inverse problems with multi-modal objectives (fitness). The search of the Pareto set (or its connected parts) is performed by applying a particular type of rank selection (*cf.* MOGA [9]), supplemented with the rank modification rule boosting fitness for parameters $\omega \in \mathcal{D}$, for which most misfits achieve sufficiently small values. Such approach can significantly improve results obtained by solving a single-objective problem with scalarization of a misfit vector $f(d, u(\omega))$.

The proposed strategy is exemplified by solving a real-world engineering problem consisting of inverting magnetotelluric (MT) measurements (see [18]) in order to characterize oil deposits located about 3 km under the Earth's surface. In this problem, two misfit functions are related

to distinct frequencies of the electric and magnetic waves, for which the maximum sensitivity with respect to the search parameter, the impedance, is expected.

2 Multi-Objective Hierarchic Memetic Search

2.1 Hierarchic Memetic Search

This section contains a short description of HMS, concentrating on its computational aspects. For the details on the system architecture and algorithms, we refer the reader to [17] and [18].

As a global optimization tool, HMS combines high-level exploratory capabilities with the accuracy and efficiency of a local optimization method. In contrast to classical two-phase methods, in which the global search phase precedes a series of local search runs, HMS intermixes local optimization executions with a global stochastic search machinery. The global part follows the multi-population evolutionary approach introduced by the Hierarchic Genetic Search (HGS) [16]. Namely, the global search is performed by a collection of genetic populations. The populations can evolve in parallel, but they are not mutually independent. The structure of the dependency relation is hierarchical (*i.e.* tree-like, see Fig. 1) with a restricted number of levels. Such a multi-population structure shows considerable exploratory capabilities combined

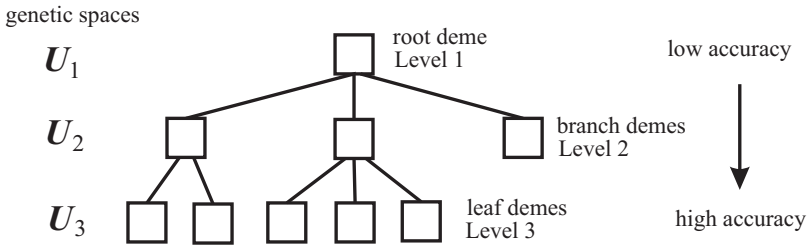

Figure 1: HMS evolutionary population tree

with a good search accuracy [21]. HMS inherits these abilities, and at the same time, it goes beyond the HGS in some important aspects. First of all, it adds local optimization to the set of operations applied to the genetic individuals. But this is done with care in order to avoid the premature population convergence and the high cost of running instances of a local method from inappropriate points. Namely, some genetic individuals (but not necessarily all of them) receive an identity and some intelligence, hence becoming independent agents in a multi-agent system (MAS), and the decision of performing the local search becomes their own responsibility. In order to turn a passive genetic individual into an intelligent one, we have to redefine the genetic operations in such a way that they can be applied to agents. This is straightforward in the case of the mutation and the crossover, but the agent selection cannot be performed in the simple genetic (or evolutionary) way. Instead, we follow the lines of the Evolutionary Multi-agent Systems (EMAS) [4], thus performing an operation analogous to the proportional or tournament selection, but realized as a two-agent rendezvous. It should be noted that the agent orientation is not the only option. In the current implementation, the active individuals are used only at the leaf level, where the search is most accurate. Therefore, the local optimization can be executed only at this level. Higher, hence less accurate, tree level demes are endowed with simple evolutionary populations. However, the demes themselves have

corresponding manager agents. Thus, the overall HMS structure is agent-based. This allows for a relatively easy and effective processing of the parallel evolution and synchronization of demes, and the distribution of decisions on the execution of the local method.

Genetic individuals located at the tree levels close to the root perform the chaotic and inaccurate search, whereas going towards the leaves the search becomes more and more focused and the accuracy is increased (see Fig. 1). The variability of the search accuracy results from the diversity of the genotype encoding precision used at different tree levels. The latter depends on the encoding type. In the case of the binary encoding (as in the Simple Genetic Algorithm), it can be achieved by the binary genotype length variation, whereas in the case of the real number encoding (as in the Simple Evolutionary Algorithm), it can be realized by the appropriate phenotype scaling. The latter case is used in the current implementation of the HMS so we present here some details. The description is based on [21, 13].

In the real number encoding, both phenotypes and genotypes are vectors from $\mathbb{R}^N$. We assume that the solution domain is a box $\mathcal{D} = [a_1, b_1] \times \cdots \times [a_N, b_N]$ and we take a sequence of scaling factors $\eta_i \in \mathbb{R}$ such that $\eta_1 > \eta_2 > \ldots \eta_{m-1} > \eta_m = 1$. Then, the genetic universum at the tree level j is $U_j = [0, (b_1 - a_1)/\eta_j] \times \cdots \times [0, (b_N - a_N)/\eta_j]$ and the encoding mapping at the level j is defined as $code_j : \mathcal{D} \ni \omega \to \{(\omega_k - a_k)/\eta_j\}_{k=1,\ldots,N} \in U_j$. Moreover, we define the scaling mapping $scale_{i,j} : U_i \ni \omega \to (\eta_i/\eta_j)\omega \in U_j$ that, in particular, enable to adopt the objectives (misfit functions) to each level of the HGS tree $f^i_m = f^i, f^i_j(x) = f^i(code^{-1}_j(x)), x \in U_j, j < m$. In such genetic universa, the search at lower levels is more chaotic (because the mutation acts stronger) and less precise (the loss of precision is caused by limitations in the real number representation). One can use various genetic operators in such an encoding. We employ both the normal mutation and the arithmetic crossover. The selection operator is described in the next subsection. A newly sprouted deme's population is sampled according to the N-dimensional Gaussian distribution centred at the properly encoded fittest individual of the parent process with the diagonal covariance matrix with values $(\sigma^{sprout}_j)^2$ on the diagonal. The sprout cannot be performed in population P at level j if there exists a population P' at level $j+1$ such that $|\overline{y} - scale_{i,i+1}(y)| < c_j$, where y is the best individual in P, $\overline{y}$ is the average phenotype of P' and c_j is a branch comparison constant.

The variable-accuracy approach of HMS allows us to take advantage of one more solved inverse problem feature. When the dependency of the forward problem solution upon the parameters is Lipschitz continuous and the objectives are computed by means of an adaptive Finite Element solver (*hp*-FEM) (see [7] for details), we can adapt the solver accuracy to the assumed accuracy of HMS tree demes. Each objective $f^i_j(x), i = 1, \ldots, n$ can be computed at the particular level j of the HMS tree in the following way:

1: solve a forward problem $A^i(u(code^{-1}_j(x))) = 0$ by *hp*-FEM for coarse and fine meshes
2: compute relative *hp*-FEM error e_{rel}
3: **while** e_{rel} is less than a level-dependent $Ratio^i(j)$ **do**
4: perform one step of *hp* adaptation
5: solve $A^i(u(code^{-1}_j(x))) = 0$ by *hp*-FEM for a new fine mesh and compute a new e_{rel}
6: **end while**
7: **return** approximate objective $f^i_j(x)$ computed using the final mesh

where the parameter $Ratio^i(j)$ depends on the Lipshitz constant of the functional f^i, and the encoding accuracy at the j-th level of the *hp*-HMS tree. Note that the aforementioned Lipschitz continuity is not obvious and it has to be proved for each particular case. For the MT problem considered here, this was proven [18, Remark 1]. Furthermore, in a few important cases, we know the dependency between the solver accuracy and the computational cost of the forward problem solution (cf. [2, 12]), which is the main unit term of the overall HMS computational

cost. Hence, by modulating the deme accuracy, we can optimize this overall cost.

2.2 Multi-objective selection and rank modification

A multi-objective version of HMS, denoted as MO-HMS, utilizes a multi-objective selection operator based on the Pareto-dominance ranking procedure proposed by Fonseca and Fleming in [9]. First, the rank of an individual is given as the number of solutions by which it is dominated in a particular deme. Second, the population is sorted according to ranks and new fitnesses are assigned according to some increasing function, so that individuals with the lowest ranks obtain the lowest (best) fitness values, and individuals with the highest ranks obtain the highest (worst) fitness values. Individuals with the same rank should obtain equal fitnesses to be sampled at the same rate.

Third, we apply *rank modification* (RM), which allows to incorporate information about the incidence between the objectives to the final fitness. RM can be used when the domains of the composing physical models that induce objective functions are the same. Let us define modified fitness function $mod\_fitness_j : U_j \to \mathbb{R}_+ \cup \{0\}$ for an individual $x \in U_j$ in a particular epoch:

$$mod\_fitness_j(x) = \frac{rank(x)}{\mu_j} + h_j(x), \tag{2}$$

where $\mu_j < +\infty$ is the population cardinality, U_j the genetic universum, and $h_j : U_j \to \mathbb{R}_+ \cup \{0\}$ is the rank modification function on the j-th level of the HMS tree. This function determines the incidence between the objectives and increases the rank of an individual, if the objective values for that individual differ considerably. In this paper, we use the following two-criteria RM function:

$$h_j(x) = c \left[\frac{f_j^1(x)}{\bar{f}_j^1} - \frac{f_j^2(x)}{\bar{f}_j^2} \right]^2, \tag{3}$$

where f_j^i, $i = 1, 2$ are the objective functions induced by two physical models, $\bar{f}_j^i$, $i = 1, 2$ are the maximum observed values of objectives on the j-th level of the HMS tree, and $c \in \mathbb{R}_+$ is a constant scaling parameter.

The fitness function for incidence-based rank modification is defined as the following:

$$fitness_j(x) = \begin{cases} mod\_fitness_j(x) & \text{if} \quad 0 \leq mod\_fitness_j(x) \leq 1 \\ 1 & otherwise. \end{cases} \tag{4}$$

The proposed RM approach allows to decrease the number of sprouted demes in parts of the Pareto front in which the incidence between objective functions is low. It also filters out solutions resulting from artifacts and model inaccuracies. Thus, the computational complexity is reduced and the number of objectives remains unchanged (*cf.* additional incidence criterion for multiple physics models with different domains introduced in [11]).

We utilize a proportional selection, where the selection probability of an individual is obtained from its fitness by using a decreasing validating function. The selection pressure can by modified by using different validating functions (see *e.g.* [10]), and incidence pressure is steered by parameter c in (3) or by changing the rank modification function.

3 Twin Objective Magnetotelluric Data Inversion

3.1 Magnetotelluric inverse problem

The MT technique is used to recover a resistivity map of the Earth's subsurface by performing electromagnetic measurements with devices located on the Earth's surface or on the oceans' bed. The MT technique differs from other geophysical measurement acquisition scenarios because it only uses natural electromagnetic radiation sources generated within the ionosphere, instead of human powered antennas. Thus, magnetolluric measurements are comparatively cheap, and can cover large areas. This method can be applied to hydrocarbon (oil and gas) exploration and to find suitable regions for storage of CO_2.

MT measurements are governed by Maxwell's equations. When the electrical field E depends only upon two spatial variables (x, z), then two independent and uncoupled modes are derived from these equations, namely *Transverse Electric* (TE) and *Transverse Magnetic* (TM). TE mode involves (E_y, H_x, H_z) field components while TM uses (H_y, E_x, E_z), where H stands for the magnetic vector field. In this work, we focus on the TE mode and we solve the equation for $E_y(\rho)$ in a regular domain $\Omega \subset \mathbb{R}^2$, assuming a distribution of the electrical resistivity ρ which belongs to the set $\mathcal{D} = \{\xi \in L^\infty(\Omega);\ \xi(x) = \sum_{i=1,\ldots,K} \xi_i \chi_i(x),\ 0 < \xi_i^{min} \leq \xi_i \leq \xi_i^{max} < +\infty\}$, where $\{\chi_i\}_{i=1,\ldots,n}$ are the indicator functions of a disjoint covering $\{\Omega_i\}_{i=1,\ldots,K}$ such that $\bigcup_{i=1,\ldots,K} \Omega_i = \Omega$, $\Omega_i \cap \Omega_j, i \neq j$. The goal-oriented *hp*-FEM is used for the effective simulation of the measuring process [1] resulting in the electrical field component $E_y(\rho)$ in Ω.

Our aim is to obtain the impedance, a suitable physical magnitude to perform the inversion. To do so, the magnetic field is obtained from Maxwell's equations and the impedance $\mathcal{Z}$ is computed according to $\mathcal{Z} = \mathcal{Z}_{yx} = E_y/H_x,\ H_x(\rho) = (j\omega\mu)^{-1}(\partial E_y(\rho)/\partial z)$, so, the approximate impedance at each antenna $i = 1, \ldots, M$ can be computed as the nonlinear functional

$$g^i(\rho) = j\omega\mu\, L^i(E_y(\rho)) \left(L^i \left(\frac{\partial E_y(\rho)}{\partial z} \right) \right)^{-1}, \quad L^i(v) = \frac{1}{\text{meas}(B^i)} \int_{B^i} v, \tag{5}$$

where B^i is a small regular neighborhood surrounding each receiver $i = 1, \ldots, M$. The Euclidean norm of a difference between measured and simulated impedances at all antennas constitutes a typical misfit in the MT inverse problem:

$$f(d, E_y(\rho)) = \frac{1}{2M} \sum_{i=1}^{M} \left| g^i(\rho) - d_i \right|^2, \tag{6}$$

where d_i are the impedances measured at each antenna $i = 1, \ldots, M$. Notice that the above misfit function is associated with the particular wave frequency for which the impedances d_i are observed.

The details of forward problem formulation, its solution using goal oriented *hp*-FEM and the dependence between forward and inverse error that allows for the effective application of *hp*-HMS stochastic inversion was studied in [18].

The frequency range is 10^{-5}–10^3 Hz, which allows to acquire measurements with a resolution that ranges from a few meters to hundreds of kilometres. The frequency also affects the depth at which the resistivity is recognized with the higher accuracy (see *e.g.* [20]). The sensitivity of the probe depends also upon the frequency, usually achieving more than one maximum [1].

We performed computations leading to restoring a subsurface resistivity in an area of about 2500 km of diameter and a depth of 0–40 km, using measurements from 7 probes located centrally, on the Earth's surface (see Fig. 2). For this particular geological model, the measurements $d^i = \{d_j^i\}$ were recorded at two frequencies, namely 10^{-3} and $10^{-1.2}$ Hz for $i = 1, 2$,

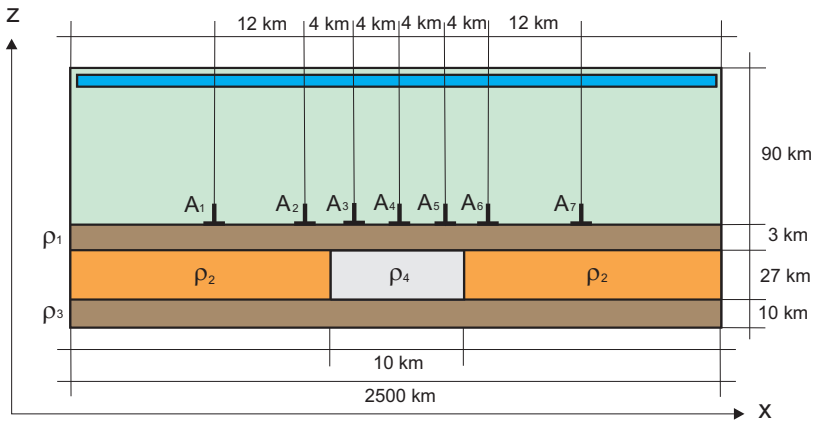

Figure 2: Geological formations and and receivers location

respectively and for all receivers $j = 1, \ldots, 7$. Such setting makes the best measurement conditions concerning both: the maximum probe sensitivity and the best penetration for a depth range 5–30 km (see [1]). The computing domain Ω is a vertical rectangle of length 2500 km and height 40 km, which is decomposed into four subdomains Ω_i, $i = 1, \ldots, 4$: upper brown, orange, lower brown and grey respectively, with a constant resistivity distributions inside (see Fig. 2). We will use two impedance misfits $f^i(d^i, E^i_y(\rho))$, $i = 1, 2$ of the same form (6) associated with the frequencies $\omega_1 = 10^{-3}$ Hz and $\omega_2 = 10^{-1.2}$ Hz mentioned above. Both criteria use the same domain $\mathcal{D}$, which is the admissible set of resistivities on the modelling area. All above settings were sufficient to formulate the Pareto problem (1) which intends to restore resistivities $\rho_1, \ldots, \rho_4$, and to apply MO-HMS with rank modification described in Sections 2.1, 2.2 for its solution.

3.2 Computational results

In our simulations, we computed the impedance by means of a goal-oriented *hp*-FEM solver (see [1] and [7] for details). Its great advantage is the ability to compute the impedance along with its first partial derivatives in a single run. For both considered frequencies, we imposed three solver accuracy levels: 60%, 20% and 3.5%, where the accuracy was measured as the maximal relative FEM error percentage. The reference impedance vectors d^1, d^2 for both misfit functions were obtained by solving the forward problem with the best available solver accuracy (3.2% for ω_1 and 1.2% for ω_2), assuming the real values $\rho_1 = 1.0$, $\rho_2 = 2.0$, $\rho_3 = 3.0$, $\rho_4 = 10.0$. HMS has three-level deme layout with Evolutionary Agents endowed with rank-modifying MO selection at every level. The computations were quite expensive, as a single HMS run lasted about three days. Therefore, the simulations were executed only five times. Each run was stopped after 20 root deme metaepochs. Other HMS execution parameters are summarized in Table 1. It turned out that the average time of FEM computations were about: 1 min 5 s (ω_1) and 1 min 35 s (ω_2) for accuracy level 60%, 2 min 10 s and 4 min 5 s for accuracy level 20%, and 3 min 5 s and 5 min 20 s for accuracy level 3.5%. The reason of differences in execution times is that for frequency ω_2, the solver had to perform more steps of *hp*-FEM adaptation to obtain the assumed accuracy. The average number of calls of each objective was: 453.4 for accuracy 60%,

Table 1: HMS execution parameters

	Root	Middle	Leaf
Population (initial)	20	10	5
Metaepoch length	2	2	2
Encoding scale	16384.0	128.0	1.0
Mutation rate	0.2	0.05	0.01
Crossover rate	0.5	0.5	0.5
Mutation std. dev.	3.0	0.6	0.1
Sprout std. dev.	-	1.0	0.2
Sprout min. dist.	-	1.0	0.2

573.4 for accuracy 20% and 233.4 for accuracy 3.5%. Therefore, the total average number of objective evaluations was $2 \cdot 1260.2 = 2520.4$.

After the end of the computations, we selected the union of all obtained leaf populations, and evaluated the modified fitness (2)-(4) in this set of individuals. In Fig. 3 we show the objective values of three categories of these individuals. The categories are determined by the modified fitness level. The fittest (red-square-marked) points form an approximation of the Pareto front. Some points do not fit in the picture because their objectives diverge too much. Namely, one point in the middle category and four points in the worst category. Tab. 2 shows

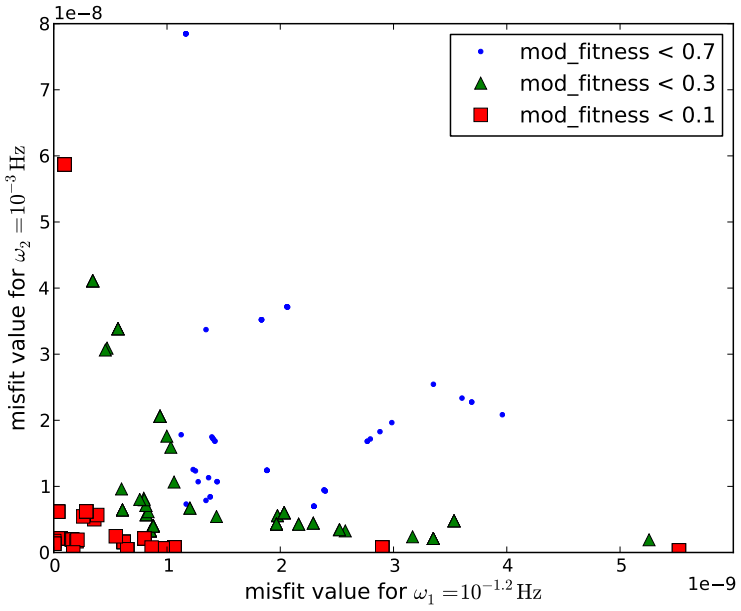

Figure 3: MT problem: Fittest points (objective space)

the 10 best individuals from the final combined population ordered according to the decreasing value of the modified fitness, given by equations (2), (3).

Table 2: Ten fittest individuals

ρ_1	ρ_2	ρ_3	ρ_4	f^1	f^2	mod. fitness
1.13084	1.89134	4.95361	3.79417	4.36966e-12	1.3282e-09	3.233923e-10
1.00934	3.35482	7.20712	5.61759	1.72058e-10	1.00846e-11	5.734588e-10
1.01717	0.861847	1.11798	5856.51	6.47885e-10	4.8077e-10	0.003891
1.14103	3827.59	555.283	0.938879	5.52019e-09	3.20812e-10	0.003892
1.15335	1.88267	5.06596	4.00167	4.6676e-12	1.733e-09	0.0116732
0.840196	1.51921	809.341	173.729	1.64577e-10	1.93778e-09	0.015564
0.848216	1.36373	930.981	153.274	2.01386e-10	1.69992e-09	0.015564
0.839527	1.53301	799.904	175.562	1.61933e-10	1.95819e-09	0.015564
0.837674	1.57199	774.275	180.752	1.55012e-10	2.01536e-09	0.015564
0.807628	1.59017	95.1825	1.01592	4.55766e-11	2.06576e-09	0.015564

4 Conclusions

The paper contains a multi-objective approach for solving challenging IPs. The objectives are misfits for the particular physical descriptions of the phenomenon under consideration (multi-physics approach), while their domain is a common set of admissible parameters. The search of the Pareto set (or its connected parts) is performed by a complex, multi-deme HMS with a particular type of rank selection, supplemented with the rank modification rule boosting fitness for parameters for which most misfits achieve sufficiently small values.

Taking into account more information coming from many physics (multiphysics) we obtain more reliable solutions than in a single physics case. Moreover, the obtained Pareto solutions or parameters close to the Pareto set deliver various possibilities of minimizing individual misfits. Finally, the selection mechanism penalizing misfit discrepancy (2)-(4) narrows the set of alternatives to the ones that are sufficiently coherent. It is still much more robust than the solution obtained for an arbitrary scalarization of a misfit vector. The applied *hp*-HMS twin adaptive strategy equipped with the common inverse and forward errors scaling and with the rank modification, allows for a moderate computational cost of this complicated strategy.

The proposed strategy is exemplified by solving a real-world engineering problem consisting of inverting MT measurements in order to characterize oil deposits located about 3 km under the Earth's surface. The results confirm that each objective delivers independent information on the solved problem. Even after rank modification, we obtain solutions with differently balanced misfits. Numerical results also show that the problem is much more sensitive to shallow and vast ground layer resistivities than to deep or narrow layer ones, as physically expected.

References

[1] J. Álvarez-Aramberri, D. Pardo, and H. Barucq. Inversion of magnetotelluric measurements using multigoal oriented *hp*-adaptivity. *Procedia Computer Science*, 18:1564–1573, 2013.

[2] B. Barabasz, E. Gajda-Zagórska, S. Migórski, M. Paszyński, R. Schaefer, and M. Smołka. A hybrid algorithm for solving inverse problems in elasticity. *International Journal of Applied Mathematics and Computer Science*, 24(4):865–886, 2014.

[3] N. Brown, B. McKay, and J. Gasteiger. A novel workflow for the inverse QSPR problem using multiobjective optimization. *Journal of Computer-Aided Molecular Design*, 20(5):333–341, 2006.

[4] A. Byrski, R. Schaefer, M. Smołka, and C. Cotta. Asymptotic guarantee of success for multi-agent memetic systems. *Bulletin of the Polish Academy of Sciences: Technical Sciences*, 61(1):257–278, 2013.

[5] S. Carcangiu, P. Di Barba, A. Fanni, M.E. Mognaschi, and A. Montisci. Comparison of multi-objective optimisation approaches for inverse magnetostatic problems. *COMPEL: The International Journal for Computation and Mathematics in Electrical and Electronic Engineering*, 26(2):293–305, 2007.

[6] N. Chakraborti, A. Shekhar, A. Singhal, S. Chakraborty, and R. Sripriya. Fluid flow in hydrocyclones optimized through multi-objective genetic algorithms. *Inverse Problems in Science & Engineering*, 16(8):1023–1046, 2008.

[7] L. Demkowicz. *Computing with hp-Adaptive Finite Elements I: One and Two Dimensional Elliptic and Maxwell Problems*. Applied Mathematics and Nonlinear Science. Chapman & Hall/CRC, 2006.

[8] H.W. Engl, M. Hanke, and A. Neubauer. *Regularization of Inverse Problems*, volume 375 of *Mathematics and its Applications*. Springer-Verlag, Berlin Heidelberg, 1996.

[9] C. Fonseca and P. Fleming. Genetic algorithms for multiobjective optimization: Formulation, discussion and generalization. In *Proceedings of the 5th International Conference on Genetic Algorithms*, volume 93, pages 416–423, San Mateo, CA, USA, 1993.

[10] E. Gajda, R. Schaefer, and M. Smołka. Evolutionary multiobjective optimization algorithm as a markov system. In R. Schaefer, C. Cotta, J. Kołodziej, and G. Rudolph, editors, *Parallel Problem Solving from Nature - PPSN XI*, volume 6238 of *Lecture Notes in Computer Science*, pages 617–626. Springer, 2010.

[11] E. Gajda-Zagórska and R. Schaefer. Multiobjective hierarchic strategy for solving inverse problems. In *IPM 2013 : proceedings of the ECCOMAS international conference on Inverse Problems in Mechanics of structures and materials*, pages 55–56. Rzeszów University of Technology Press, 2013.

[12] E. Gajda-Zagórska, R. Schaefer, M. Smołka, M. Paszyński, and D. Pardo. A hybrid method for inversion of 3D DC logging measurements. *Natural Computing*, 2014. available at `http://dx.doi.org/10.1007/s11047-014-9440-y`.

[13] P. Jojczyk and R. Schaefer. Global impact balancing in the hierarchic genetic search. *Computing and Informatics*, 28(2):181–193, 2009.

[14] K. Miettinen. *Nonlinear Multiobjective Optimization*. Kluwer Academic Publishers, Boston, USA, 1999.

[15] M. Preuss, G. Rudolph, and T. Feelly. Solving multimodal problems via multiobjective techniques with application to phase equilibrium detection. In *Proceedings of the IEEE Congress on Evolutionary Computation, 2007, CEC 2007*, pages 2703–2710, 2007.

[16] R. Schaefer and J. Kołodziej. Genetic search reinforced by the population hierarchy. In *Foundations of Genetic Algorithms 7*, pages 383–399. Morgan Kaufman, 2003.

[17] R. Schaefer and M. Smołka. A memetic framework for solving difficult inverse problems. In *EvoApplications 2014*, volume 8602 of *Lecture Notes in Computer Science*, pages 138–149. Springer, 2014.

[18] M. Smołka, R. Schaefer, M. Paszyński, D. Pardo, and J. Álvarez-Aramberri. Agent-oriented hierarchic strategy for solving inverse problems. *International Journal of Applied Mathematics and Computer Science*, 25(3), 2015. to appear.

[19] A. Tarantola. *Inverse Problem Theory*. Mathematics and its Applications. Society for Industrial and Applied Mathematics, 2005.

[20] K. Vozoff. The magnetotelluric method in the exploration of sedimentary basins. *Geophysics*, 37(1):98–141, 1972.

[21] B. Wierzba, A. Semczuk, J. Kołodziej, and R. Schaefer. Hierarchical Genetic Strategy with real number encoding. In *Proceedings of the 6th Conference on Evolutionary Algorithms and Global Optimization*, pages 231–237, 2003.